Suppressing and amplifying neural oscillations in real-time using phase-locked electrical stimulation: concept, optimization and in-vivo testing

David Escobar Sanabria[1], Luke A. Johnson[1], Ying Yu[1], Zachary Busby[1], Shane Nebeck[1], Jianyu Zhang[1], Noam Harel[2], Matthew D. Johnson[3], Gregory F. Molnar[1], Jerrold L. Vitek[1*]

[1] Department of Neurology, University of Minnesota, Minneapolis, MN, USA

[2] Department of Radiology, University of Minnesota, Minneapolis, MN, USA

[3] Department of Biomedical Engineering, University of Minnesota, Minneapolis, MN, USA

* Correspondence should be addressed to J.L.V. (vitek004@umn.edu) or D.E.S. (descobar@umn.edu)

Abstract

Approaches to predictably control neural oscillations are needed to understand their causal role in brain function in healthy and diseased states and to advance the development of neuromodulation therapies. In this article, we present a neural control approach and optimization framework to actively suppress or amplify neural oscillations observed in local field potentials in real-time by using electrical stimulation. The rationale behind this control approach is that neural oscillatory activity evoked by electrical pulses can suppress or amplify spontaneous oscillations via destructive or constructive interference when stimulation pulses are continuously delivered at precise phases of these oscillations in a closed-loop scheme. We demonstrate that this technique, referred to as phase-locked brain stimulation, is capable of actively suppressing or amplifying 8-17 Hz oscillations in the subthalamic nucleus of two parkinsonian nonhuman primates, which exhibited a robust increase in oscillatory power in this frequency band following administration of the neurotoxin MPTP (1-methyl-4-phenyl-1,2,3,6-tetrahydropyridine).

Introduction

Neuromodulation approaches that predictably control circuit-level neural dynamics in real-time will be of utility in neuroscience to deductively infer causal relationships between controlled changes in these dynamics and brain function. These control approaches could also help identify neural processes causally linked to the manifestation of brain conditions and inform the development of neuromodulation therapies. Neural dynamics observed from local field potentials (LFPs) are of particular interest to the development of neuromodulation therapies with feedback (closed-loop) given the long-term stability of LFP recordings in cortical

and subcortical brain structures in human subjects [1,2]. Evidence from experimental studies and computer simulations suggest that LFPs at low-frequency (<100 Hz) are generated predominantly by synchronized synaptic inputs to neuronal ensembles near the recording site[3,4]. Controlling synchronized synaptic activity in a targeted neuronal ensemble can therefore help modulate information flowing into the target, and thereby influence the information flowing out of the target. Feedback (closed-loop) control systems can drive the dynamics of complex systems to a desired state by adjusting inputs (actuation) based on real-time measurements of the controlled system dynamics (sensing). These feedback control technologies offer the ability to control neural processes by using LFP data as a feedback signal and electrical stimulation for actuation[5].

On-demand brain stimulation, a form of feedback control, has been used in patients with epilepsy and Parkinson's disease (PD) to deliver isochronal (fixed-frequency) electrical pulses based upon neurophysiological signals extracted from LFP data. In epilepsy patients, isochronal pulse trains have been delivered in response to detection of inter-ictal epileptiform activity using LFP data and have been able to reduce the likelihood of seizure onset while minimizing the amount of time in which stimulation is delivered to the brain[6]. In PD, high-frequency isochronal stimulation has been delivered to the subthalamic nucleus (STN) on demand based on the power of beta band (13-30 Hz) oscillations, which are thought to underlie the development of bradykinesia and rigidity[7]. Because these therapies are delivered on demand, they can minimize the amount of stimulation energy delivered to the brain and likelihood of potential side effects that may occur with continuous stimulation as a result of current spread beyond the targeted region. They are not designed, however, to increase the efficacy of isochronal stimulation or reshape the dynamics of brain circuitry, mainly because the mechanisms by which isochronal stimulation alters brain activity and function are not well

understood.

A recent study showed that open-loop, isochronal, low-frequency stimulation delivered dorsal of the STN in PD patients could alter the amplitude of low-frequency oscillations recorded in the STN, whenever consecutive stimulation pulses landed at specific phase angles of these oscillations[8]. This study points out that stimulation phase-aligned to neural oscillations and delivered in a closed-loop scheme could potentially be used to modulate LFP oscillations. However, the mechanisms by which low-frequency stimulation modulates LFP oscillations and the rationale to implement phase-locked stimulation in a closed-loop scheme are not clear. Clarifying these mechanisms and rationale could help us develop a feedback control approach to actively modulate neural oscillatory activity in a more precise and predictable fashion.

In this study, we developed and tested in-vivo a feedback control framework to actively suppress or amplify spontaneous neural oscillations in real-time by using LFP measurements for sensing and electrical stimulation for actuation. The rationale behind this control approach and our working hypothesis is that damped oscillations evoked by electrical pulses can suppress or amplify spontaneous neural oscillations via destructive/constructive interference when stimulation pulses are continuously delivered at precise phases of these oscillations in a closed-loop scheme. This neural control framework, referred to as phase-locked stimulation, was tested with two parkinsonian nonhuman primates, which exhibited a robust increase in in the power of oscillations in the 8-17 Hz frequency band following administration of the neurotoxin MPTP (1-methyl-4-phenyl-1,2,3,6-tetrahydropyridine), similar to the oscillations observed in PD patients and thought to underlie the development of PD motor signs[9,10]. We were able to actively suppress or amplify STN oscillations in the studied animals by delivering stimulation in the internal segment of the globus pallidus (GPi) phase-locked to oscillations in the STN. Based on these experiments and computer simulations constructed using LFP data,

we demonstrate that the neuromodulation mechanism of phase-locked stimulation is constructive or destructive interference between stimulation-evoked oscillations and spontaneous oscillations. Additionally, we developed a methodology to optimize the parameters of phase-locked stimulation and achieve maximum amplification or suppression of neural oscillations. The neural control and optimization methodology presented in this study suggest that phase-locked stimulation can be used to systematically modulate neural oscillatory activity in real-time and control neural oscillatory dynamics in which oscillations are the fundamental block; for example, to control synchronization and coupling of neural circuits.

Results

Spontaneous neural activity can be modulated using oscillations evoked by electrical stimulation

Evidence from in-vivo and computational studies indicate that spontaneous and evoked LFP oscillations (<100 Hz) in both cortical and subcortical brain regions are generated predominantly by synchronized synaptic inputs (inhibitory or excitatory) to neuronal ensembles in these regions[3,4,11]. Low-frequency, damped, neural oscillations evoked by electrical stimulation of neural tissue have also been shown to be related to synaptic activity and generated by activation of mono- or multi-synaptic pathways originating in the stimulation site and propagating to the recording site[11–14]. The neural control approach described in this article provides a framework to modulate synaptic inputs measured via LFPs in the targeted neuronal population. See schematic in **Fig. 1a**.

Two nonhuman primates (J and P), rendered parkinsonian with the neurotoxin MPTP, were used to develop and test the phase-locked brain stimulation methodology. Animals

treated with MPTP exhibit an increase in the amplitude of oscillations in the STN in the 8-30 Hz band, similar to oscillations observed in humans with PD [15,16]. The power spectral density (PSD) plots of **Figs. 1b,c** illustrate how the power of LFPs in the STN was increased in the parkinsonian condition of the studied animals. These LFPs were created by differentiating potentials at electrode pairs of a deep brain stimulation (DBS) lead located within the STN and used for sensing in the closed-loop system. Differentiation helps minimize the effect of far field potentials and preserve information that is near the recording electrodes. Location of the DBS leads with electrodes in the STN are shown in **Supplementary Fig. 1**. The frequency bands targeted for modulation were centered at around 11 Hz in animal J and 14 Hz in animal P (**Fig. 1b,c**). Oscillatory modes in these bands were selected because of their high amplitude relative to other oscillatory modes across frequencies. A frequency range of 6 Hz around the targeted center frequencies was selected for the implementation of phase-locked stimulation to allow for variations in the frequency of oscillations while attenuating information outside the frequency band of interest.

The degree of suppression or amplification of neural oscillations that can be achieved using phase-locked stimulation depends upon the amplitude of the stimulation-evoked oscillations in the targeted frequency band. Stimulation-evoked potentials are an indirect measurement of the size of neural oscillations evoked by electrical stimulation and are used here as a proxy to quantify the effect of electrical stimulation pulses on neural activity. We selected electrode contacts estimated to be within the GPi to deliver bipolar electrical stimulation locked to the oscillations measured in the STN for two reasons. First, large evoked potentials were observed in the STN of both animals when stimulation was delivered in the GPi. Second, stimulation in the GPi resulted in smaller stimulation-induced artifacts in the STN than those observed when stimulation was delivered within the STN itself. Reducing the size of

stimulation-induced artifacts facilitated the suppression of these artifacts in real-time and improved the quality of recordings.

We characterized the temporal dynamics of stimulation-evoked potentials in the STN by delivering low-frequency (<4 Hz) anodal and cathodal stimulation to the GPi, computing stimulation triggered averages of the LFP time series in the STN for both anodal and cathodal stimulation ($X_a(t)$ and $X_c(t)$), and calculating the mean between the anodal and cathodal responses ($(X_a(t) + X_c(t))/2$). This mean evoked response attenuates the stimulation artifacts while preserving the neural evoked potential[17]. The stimulation-evoked potentials in the STN are shown in **Fig. 1d,e**. A more detailed characterization and mathematical model of the evoked potentials are presented in the **Supplementary characterization and mathematical modeling of stimulation evoked oscillations**. The amplitude of the stimulation pulses used to characterize evoked potentials and implement the phase-locked stimulation technique in animal J and P was below 800 μA, which was below the stimulation threshold at which we observed side effects associated with activating the internal capsule (e.g. muscle contractions).

The amplitude of neural oscillations was a function of the stimulation phase

By using the closed-loop brain stimulation framework described above, we were able to modulate low-frequency neural oscillations in the STN of animal J and P. In both animals, the amplitude of the neural oscillations in the targeted frequency bands was a function of the phase angle at which a train of stimulation pulses was delivered (**Figs. 2a-d**). A single pulse was delivered at each oscillatory cycle in animal P, whereas a train of 3 pulses (165 Hz intra-burst rate) was used in animal J to enhance the modulatory effect of the pulses via temporal summation. The first pulse of the train was aligned to the targeted phase estimate The results

also show that there are unique phase angles for which maximum amplification or suppression of neural oscillations can be achieved. The lag between these angles was 180 degrees.

The amplitude of the targeted oscillations, when maximum amplification or suppression were achieved, was significantly different from the amplitude of oscillations when stimulation was OFF with $p<0.05$ (**Fig. 3**). The degree of amplification was higher than the degree of suppression in the experiments. One reason for this difference is that stimulation was discontinued when the amplitude envelope of the oscillations was below the 25th percentile threshold. The angles associated with the maximum suppression for animal J and P were 135 and 35 degrees, respectively. The angles associated with the maximum amplification for animal J and P were -45 and -145 degrees, respectively.

Short duration and latency evoked oscillations did not play a role in the modulation of low-frequency oscillations

Short duration (<3 ms) and short latency (<3 ms) components of the evoked potentials have been shown to be associated with antidromic activation of neuronal ensembles[18]. Short duration and latency evoked oscillations, likely associated with antidromic activation of the STN, were observed in our data (**Figs. 1d,e**). These short-latency signal components are, however, not associated with the low-frequency synaptic activity that we want to measure and modulate, and had a negligible effect on the spectral measurements at low-frequency bands due to their low power in these bands.

Modulation was local and not artefactual

In both subjects, the degree of modulation across different contact pairs in different

regions inside and outside of the STN was not correlated with the size of the stimulation-induced artifacts, indicating that artifacts did not influence the observed modulation (**Figs. 2c,d**). Additionally, evoked potentials measured with electrodes estimated to be within the STN were larger than those outside the STN, suggesting that evoked neural activity was generated by neural sources and sinks located near electrodes located within the STN. Spontaneous oscillations in the 8-30 Hz exhibited larger amplitudes inside the STN than outside (OFF state in **Fig. 2c,d**). Furthermore, the degree of amplification or suppression of spontaneous oscillations achieved when phase-locked stimulation was delivered was larger in electrodes located within the STN.

Computer simulations can approximate the steady-state effect of evoked neural activity on neural modulation

Mathematical models of the evoked potentials and steady-state computer simulations of the closed-loop system were constructed based on experimental data to estimate the stimulation phase and amplitude that is predicted to optimally amplify or suppress neural oscillations using phase-locked stimulation. The temporal dynamics of evoked potentials were characterized using linear, time-invariant differential equations and parameterized via system identification techniques[19]. A more detailed description of the evoked potential characterization and mathematical models is presented in the **supplementary characterization and mathematical modeling of stimulation evoked oscillations** and **Supplementary Fig. 2**. Evoked potentials were observed when the stimulation amplitude was greater than or equal to a non-zero value (lower bound). The amplitude of these evoked potentials was a linear function of the stimulation amplitude for stimulation amplitudes greater than the lower bound at which evoked responses occurred. The input-output relationship between the stimulation pulse and evoked

potential is accurately characterized by the mathematical models as shown in **Figs. 4a,b** and **Supplementary Fig. 2**. By using the mathematical models of the evoked potentials, numerical simulations were created in which the closed-loop algorithms were evaluated. The numerical simulations incorporated the same algorithms, filters, and time delays present in the real-time control computer to predict optimal stimulation phase angles that suppress or amplify oscillations. In these computer simulations, simulated evoked potentials as well as computer-generated sinusoidal oscillations (synthetic) or previously recorded LFP data were added to obtain the modulated potential.

Simulations of the closed-loop stimulation system and algorithms were created using recorded LFP data in the off-stimulation state to assess whether the mathematical model approximates the experimental data in which phase-locked stimulation was delivered to the animals. A computer simulation of the experiment shown in **Fig. 4d** was created using LFP data in the stimulation-off condition and is shown in **Fig. 4e**. The computer-generated data reproduces the changes in oscillatory power as a function of stimulation phase observed in the in-vivo experiment (**Fig. 4d** vs **Fig. 4e**). This similarity provides evidence of the modulatory role of stimulation-evoked oscillations in the phase-locked stimulation framework. The computer simulations do not reproduce or exhibit stimulation-induced artifacts, further providing evidence that the modulations are mediated by neurophysiological oscillations evoked by stimulation, but not by stimulation-induced artifacts. Discrepancies between simulation and experimental data can be attributed to temporal dynamics and nonlinearities present in the neural circuits but not captured in our steady-state computer simulations.

Optimal modulation parameters can be estimated using data-driven models of the evoked potentials

Finding stimulation phase angles and amplitudes to maximize the amplification or suppression of neural oscillations is a goal for using phase-locked stimulation. This problem is, however, intractable experimentally due to the large parameter space (stimulation phases and amplitudes) and complexity of the experiments. We addressed this problem through computer simulations based upon the data-driven mathematical models of stimulation-evoked potentials (**Section 2.3**). We used sinusoids with an amplitude equal to the mean amplitude of experimentally recorded STN oscillations as a synthetic LFP signal in the computer simulation. Stimulation was delivered at various phase angles (-175, -170, 165, …, 180 deg) and stimulation amplitudes (300, 350….,750, 800 μA) in the computer simulations and a search was performed to calculate the optimal phases and amplitudes that resulted in maximum suppression or amplification of the oscillations in the targeted frequency band. The amplitude envelope of the modulated signal in the targeted frequency band was then used to quantify the degree of modulation achieved using phase-locked stimulation in these computer simulations. The optimal stimulation amplitude to amplify oscillations is equal to the maximum amplitude (upper bound) employed in the search since the size of the evoked potentials is proportional to the stimulation amplitude in both the mathematical models and experimental data[17,18]. See **supplementary characterization and mathematical modeling of stimulation evoked oscillations** and **Supplementary Fig. 2**. The optimal amplitude to suppress oscillations is not necessarily equal to the optimal stimulation amplitude to amplify oscillations since evoked oscillations with high amplitude can create constructive interference even when delivering stimulation at phase angles at which suppression is achieved at lower stimulation amplitudes. A more detailed description of the optimization approach is described in the **supplementary optimization approach**. We applied the search approach described above to estimate the optimal stimulation phase and amplitude to suppress/amplify 11-17 Hz oscillations in animal P by using one single stimulation pulse. The optimization considered the mean amplitude of the

oscillations envelope measured in the resting, off-stimulation state of the animal. A map of the optimization search, with values of the mean amplitude of the oscillations envelope after phase-locked stimulation is applied in the computer simulations at different phases and amplitudes, is shown in **Fig. 5a**.

The optimal phase and amplitude to suppress oscillations were found to be 35 deg and 600 μA, respectively. The optimal phase angles for both suppression (35 deg) and amplification (-145 deg) of oscillations at a fixed stimulation amplitude of 600 μA were the same found experimentally in the experiment depicted in **Figs. 2b** and **Fig. 3c.** These stimulation parameters were used in an experiment with the animal, in which we alternated between maximum suppression and amplification of neural oscillations (**Fig. 5b**). The results of and data shown in **Figs. 2b,d** and **Fig. 5b** validate the search approach utilized to optimize the stimulation phase and amplitude and illustrate the capability of phase-locked stimulation to actively suppress or amplify neural oscillations in real-time. The experiments also show that while we attempt to modulate neural oscillations in the 11-17 Hz band, there are changes in power in higher frequency bands.

Discussion

We developed an experimental approach and optimization framework to systematically and predictably control neural oscillations recorded from LFP data in-vivo. The neural control approach, referred to as phase-locked brain stimulation, is capable of precisely suppress or amplify the amplitude of neural oscillations with the resolution and time-scale needed to characterize the functional role of oscillatory dynamics in brain circuits. The optimization framework described in this article to predict the optimal phase angles and stimulation

amplitudes that maximize the degree of suppression or amplification of targeted neural oscillations resolves a problem that is intractable experimentally. Together these neural control and optimization approaches provide researchers with tools to address fundamental questions regarding the causal role of circuit-level oscillatory dynamics in brain function and disease. We used macro-electrode arrays and electrical stimulation waveforms similar to those used in humans chronically implanted with brain stimulation systems for epilepsy and PD. Phase-locked electrical stimulation may therefore be a feasible approach to study brain function and disease directly in humans.

Modulation mechanisms of phase-locked stimulation

The rationale behind this control framework is that low-frequency oscillations can be actively overwritten (amplified or suppressed) by continuously delivering stimulation pulses at specific phases of the oscillations. The mechanism by which phase-locked stimulation exerts its effect on neural oscillatory activity is likely secondary to its effect on synaptic inputs evoked by electrical stimulation and generated by activation of mono- or multi-synaptic targeted neuronal populations and fiber pathways[11–14].

For the experiments carried out in this study, we assumed that both spontaneous and evoked low-frequency oscillations in the STN of the animals were associated with synaptic inputs innervating common STN neuronal ensembles. In the experiments, we targeted oscillations in the 8-17 Hz band in the STN of two parkinsonian monkeys. The amplitude of oscillations in this band exhibited an increase following MPTP administration. The pathophysiological mechanisms by which the amplitude of these oscillations increase in parkinsonian animals and are observed in PD patients is still being studied. Studies with the 6-OHDA mouse model of PD and computer simulations of the human STN indicate that a

combination of synchronized inhibitory and excitatory synaptic inputs from the cerebral cortex and the external segment of the globus pallidus (GPe), innervating common neuronal ensembles contributes to the development of these oscillations in the STN[20,21]. In the experiments carried out in this study, we modulated neural oscillations in the STN in the 8-17 Hz band by delivering stimulation in the GPi phase-locked to the oscillations in the STN.

This modulation was mediated by stimulation-evoked oscillations that suppressed or amplified spontaneous low-frequency oscillations in the STN. These evoked oscillations had elevated power content at the frequencies of oscillations targeted for modulation and were likely associated with synaptic inputs to the STN. Although low-frequency damped oscillations in the STN evoked by GPi stimulation have not been previously characterized, based on known anatomical connections, these evoked oscillations may emerge from a combination of one or more of the following: 1) antidromic activation of GPe branches and subsequent orthodromic activation of collateral branches connecting the GPe to the STN[22]; 2) orthodromic activation of GPi-PPN-STN pathways, and 3) orthodromic activation of pallido-thalamo-cortico-subthalamic loops. Consequently, controlled changes in the amplitude of STN oscillations achieved via phase-locked stimulation may be mediated by simultaneous synaptic inputs to neuronal ensembles in the STN, coming from multiple cortical and subcortical structures involved in the generation of spontaneous and stimulation-evoked oscillations.

Short-latency (high-frequency), short-duration evoked oscillations observed in the STN of the studied animals were likely the result of antidromic activation of the STN to GPi pathway. Therefore, they are in principle not associated with synaptic inputs to the STN. Additionally, these short-duration oscillations observed in the LFP data do not have a noticeable impact on our measurements of neural modulation in the targeted frequency bands as their power is negligible in these frequencies.

Utility of neural control approach

The neural control framework presented in this article enables a systematic and continuous suppression or amplification of neural oscillations in real-time by using electrical stimulation. This approach can be employed as a building block to deductively infer causal relationships between controlled changes in the amplitude of LFP oscillations, circuit-level brain function, and/or behavior.

The neural control framework described in this article can be leveraged to modulate and characterize the role of circuit-wide neural dynamics in which oscillations are a building block, including synchronization and coupling[23,24]. Additionally, we can employ this framework to study how controlled changes in oscillatory dynamics and related changes in circuit-wide neural activity are causally linked to the manifestation of brain conditions. Examples of indications where this neural control framework can be applied are epilepsy and Parkinson's disease. In epilepsy, one could study whether attenuating synchronized epileptiform neural activity can directly or indirectly alter the probability of seizure onset[25]. In Parkinson's disease this framework could be used to assess whether synchronization and coupling of low-frequency (5-30 Hz) oscillations throughout the basal ganglia-thalamocortical circuit are linked (directly or indirectly) to bradykinesia, rigidity, and/or tremor[9,26]. By improving our understanding of causal links between neural circuit dynamics and brain conditions, this closed-loop brain stimulation approach could also guide the development of subject specific neuromodulation therapies delivered based on LFP activity within specific regions of the brain.

From a technological standpoint, phase-locked stimulation is suitable for testing in human subjects because we use waveforms traditionally used to deliver electrical stimulation as well as LFP data for sensing. LFP data chronically recorded from cortical and subcortical

brain structures via macro-electrode arrays have been demonstrated to provide usable neurophysiological information in humans for extended periods of time[27]. The experimental setup used in this study, with sensing in the STN and stimulation in the GPi, provides a proof of concept for the implementation of phase-locked brain stimulation. The particular setup used in this study, with electrodes in both the STN and GPi, has been implemented in humans[28]; however, it's a not standard practice as DBS leads are typically implanted in one brain target within the same cerebral hemisphere. In applications in which LFPs are recorded from and stimulation is delivered to the same brain region using a single electrode array (e.g. DBS for PD), hardware and/or software technologies that enable effective and robust artifact removal in real-time are needed to rigorously implement phase-locked stimulation.

Limitations

We assumed that spontaneous and evoked LFP oscillations measured in the STN of the studied animals were associated with synaptic inputs innervating common STN neuronal ensembles. This is a reasonable assumption given that STN neurons simultaneously receive inputs from multiple structures, including the GPe and motor cortex. However, we acknowledge that spontaneous and evoked oscillations may be generated by inputs to adjacent but different populations of neurons, and modulations observed in the experiments may be the effect of the superposition of currents from different neuronal ensembles. Recordings of synaptic activity (postsynaptic potentials) and/or neuronal activity in populations of STN neurons during periods of phase-locked stimulation are needed to understand how this stimulation approach exerts its effect in the cellular level. Although cellular-level mechanisms of modulation are not experimentally addressed in this study, the conceptual framework of phase-locked stimulation, implementation scheme, and optimization method presented in this

article provide proof of concept for this neural control approach.

The degree of suppression of neural oscillations achieved using phase-locked stimulation was lower than the degree of amplification because we discontinued stimulation when the amplitude envelope of the targeted oscillations was below a threshold equal to the 25th percentile of this envelope in the off-stimulation condition. This threshold based approach was implemented to avoid delivering stimulation based on measurements close to the noise floor. A 25th percentile is, however, likely a conservative threshold that may have limited our ability to further suppress oscillations using phase-locked stimulation. Further analysis of optimal threshold selection is needed to improve the modulation effect of this technique. The experimental data shown in **Figs. 2a,b** and **Fig. 5b** indicate that phase-locked stimulation alters oscillatory activity in frequency bands not targeted for modulation. These alterations are, at least in part, due to the power content of the evoked neural activity in frequencies outside the band selected for modulation. Stimulation patterns different to constant amplitude pulse trains may be needed to reduce the activation of neural oscillatory activity in frequency bands outside that selected for modulation using phase-locked stimulation.

The relative benefit of phase-locked stimulation compared to standard brain stimulation approaches using isochronal stimulation remains to be determined, but the potential utility of this technique for both improving current stimulation therapies and for understanding the pathophysiological basis underlying circuit disorders is compelling.

Methods

Instrumentation and subjects

All procedures were approved by the University of Minnesota Institutional Animal Care

and Use Committee (IACUC) and complied with United States Public Health Service policy on the humane care and use of laboratory animals. Two adult female rhesus macaques (Macaca mulatta) were used in this study, subjects: J (17 years), P (18 years). Each animal was then implanted in both the STN and GPi with 8-contact scaled down versions of human DBS leads (0.5 mm contact height, 0.5 mm inter-contact spacing, 0.625 mm diameter, NuMED, Inc.) as previously described[15]. DBS lead locations were approximated using fused pre-implantation MRI, post-implantation CT images and histological reconstructions (**Supplementary Fig. 1**), together with microelectrode mapping of the STN and GPi prior to implantation of the leads. Data were collected in the normal and parkinsonian state of the animals. The animals were rendered parkinsonian by systemic (intramuscular) and intra-carotid injections of the neurotoxin 1-methyl-4-phenyl-1,2,3,6 tetrahydropyridine (MPTP)[29].

Neural data acquisition and electrical stimulation

Neurophysiological data in the awake-resting state were utilized to characterize how neural oscillations across frequencies changed in the STN from the normal to the parkinsonian condition. Neural data in the resting-awake state were collected using a Tucker David Technologies (TDT, Alachua, FL, USA) workstation with a sampling rate of ~24 KHz. Signals were band-pass filtered (0.5-700 Hz) to extract LFP data and down-sampled to ~3 KHz for analysis. LFPs were created by subtracting potentials from contacts estimated to be within the STN. We verified that the animals were alert using video monitoring[15].

The power of neural oscillations across frequencies was computed using power spectral densities (PSDs) and the Welch's method. To compute the PSDs, we used 214 points in the fast Fourier transform, a Hamming window of 1.34 sec (¼ 214 points), zero padding (¾ 214 points), and an overlap of 50%. The PSD curves were normalized with respect to the total

power, which is the sum of PSD values over all frequencies. The normalized power describes the proportion of power in each frequency band relative to the total power across all frequencies. Analyses were performed using customized scripts in MATLAB (Mathworks, Natick, MA, USA).

Implementation of neural control approach

We implemented phase-locked stimulation using a Tucker David Technologies (TDT, Alachua, FL, USA) neurophysiological recording and stimulation system and a computer fully dedicated to executing signal processing and control algorithms in real-time. LFP data were sampled at ~24 KHz in the neurophysiological recording system, amplified in the +/-10 V range, and transmitted to the control computer via analog channels. The analog signals were digitized in the control computer at ~24 KHz and electrical artifacts were removed from the LFP data by holding for 2.3 ms the value of the LFP sample acquired before the stimulation pulse was triggered. The 2.3 ms holding period was longer than the duration of the artifact but short enough to avoid degrading information recorded at low-frequency. The artifact-suppressed LFP data were then band-pass filtered in the frequency band selected for modulation using second-order Butterworth filters and subsequently down-sampled at 3 KHz. The instantaneous phase and amplitude of oscillations in the targeted frequency band were estimated using a Hilbert transformer filter[30]. The Hilbert filter introduced 16 samples of time delay (5.3 ms) to the closed-loop interconnection, which corresponds to a 23 deg. phase lag relative to the 11 Hz oscillations targeted in animal J and 26 deg. phase lag relative to the 14 Hz oscillations targeted in animal P. A train of stimulation pulses, three for animal J and one for animal P, were delivered at specified phase angles. whenever the amplitude envelope of the oscillations was above the 25th percentile of the envelope computed in the off-stimulation state.

Stimulation was turned off when the envelope was below threshold to avoid delivering stimulation based on measurements with small signal to noise ratio. Stimulation was delivered using bipolar, charge-balanced, biphasic, symmetric stimulation pulses with pulse widths of 80 μsec. In the bipolar configuration, the cathode and anode of the stimulation system were connected to separate contacts in the DBS lead located within the GPi. This bipolar configuration was used to minimize the size of artifacts in the recording site. Charge-balanced biphasic pulses were selected to deliver a net zero current and avoid tissue damage [31,32]. The total delay of the closed-loop interconnection, associated with hardware communication was less than 1 ms. This delay was computed as the period between the sample at which the stimulation command was sent from the real-time computer to the stimulation system and the time at which the stimulation artifact was detected in the recordings of the real-time computer. Signal processing and control algorithms were developed using Simulink Real-Time (Mathworks, Natick, MA, USA).

Quantification of neural modulation

We assessed whether the amplitude of neural oscillations changed when phase-locked stimulation was delivered by using scalar measurements of the oscillations amplitude envelope. The scalar measurements are equal to the average of the amplitude envelope over non-overlapping windows of one-second duration. The analytical amplitude of neural oscillations in the targeted frequency band was computed by filtering the raw data in this band, applying the Hilbert transform, and calculating the magnitude of the analytic signal obtained from the Hilbert transform. Pairwise differences between scalar measurements of the oscillations' amplitude in two different conditions were assessed via the Wilcoxon rank-sum test. The p-values resulting from this test were corrected for the number of comparisons via the

Bonferroni method. We assumed that the difference between measurements in the two conditions was significant when $p < 0.05$. The comparisons made were stimulation off vs amplification and stimulation off vs suppression.

Acknowledgements

Research reported in this publication was funded by the Wallin Discovery Fund, the Engdahl Family Foundation, the National Institutes of Health, National Institute of Neurological Disorders and Stroke (P50-NS098573, R01-NS037019, R01-NS077657, R01-NS110613, R01-NS094206), the University of Minnesota's MnDRIVE (Minnesota's Discovery, Research and Innovation Economy) Initiative Postdoctoral Fellowships to D.E. and L.A.J. We thank Tay Netoff for the discussions and suggestions regarding closed-loop brain stimulation techniques. We thank Claudia Hendrix, Devyn Bauer and Ben Teplitsky for their help with histology processing.

Author Contributions

D.E.S designed experiments, analyzed the data, and prepared the manuscript; L.A.J., J.Z., and Y.Y. performed surgical procedures; D.E.S., L.A.J., S.N., and Z.B. carried out the experiments; L.A.J., and M.D.J. contributed to manuscript revisions; N.H. contributed to the image (MRI and CT) acquisition and analysis, G.M. and M.D.J. provided logistical support; J.L.V participated in all aspects of the study.

Competing interests

J. L. Vitek has served as a consultant for Medtronic, Boston Scientific and Abbott.

Data availability

The datasets generated during and/or analyzed during the current study are available from the corresponding author upon reasonable request.

Code availability

The code generated during the current study is available from the corresponding author upon reasonable request.

References

1. Hanrahan, S. J. *et al.* Long-Term Task- and Dopamine-Dependent Dynamics of Subthalamic Local Field Potentials in Parkinson's Disease. *Brain Sci.* **6**, (2016).
2. Staub, F. *et al.* EP 4. Long term recordings of deep brain activity from the subthalamic nucleus in PD patients using PC+S. *Clin. Neurophysiol.* **127**, e176 (2016).
3. Buzsáki, G., Anastassiou, C. A. & Koch, C. The origin of extracellular fields and currents — EEG, ECoG, LFP and spikes. *Nat. Rev. Neurosci.* **13**, 407–420 (2012).
4. Herreras, O. Local Field Potentials: Myths and Misunderstandings. *Front. Neural Circuits* **10**, (2016).
5. Schiff, S. J., Poggio, T. A. & Sejnowski, T. J. *Neural Control Engineering: The Emerging Intersection Between Control Theory and Neuroscience*. (MIT Press, 2011).
6. Morrell, M. J. & RNS System in Epilepsy Study Group. Responsive cortical stimulation for

the treatment of medically intractable partial epilepsy. *Neurology* **77**, 1295–1304 (2011).

7. Little, S. *et al.* Adaptive deep brain stimulation in advanced Parkinson disease. *Ann. Neurol.* **74**, 449–457 (2013).
8. Holt, A. B. *et al.* Phase-Dependent Suppression of Beta Oscillations in Parkinson's Disease Patients. *J. Neurosci. Off. J. Soc. Neurosci.* **39**, 1119–1134 (2019).
9. Brown, P. Oscillatory nature of human basal ganglia activity: relationship to the pathophysiology of Parkinson's disease. *Mov. Disord. Off. J. Mov. Disord. Soc.* **18**, 357–363 (2003).
10. Ray, N. J. *et al.* Local field potential beta activity in the subthalamic nucleus of patients with Parkinson's disease is associated with improvements in bradykinesia after dopamine and deep brain stimulation. *Exp. Neurol.* **213**, 108–113 (2008).
11. Magill, P. J., Sharott, A., Bevan, M. D., Brown, P. & Bolam, J. P. Synchronous unit activity and local field potentials evoked in the subthalamic nucleus by cortical stimulation. *J. Neurophysiol.* **92**, 700–714 (2004).
12. Volkov, I. O. Unit responses in the cat auditory cortex to electrical stimulation of nerve fibers innervating receptor cells in different parts of the organ of corti. *Neurophysiology* **14**, 317–323 (1982).
13. Kumaravelu, K., Oza, C. S., Behrend, C. E. & Grill, W. M. Model-based deconstruction of cortical evoked potentials generated by subthalamic nucleus deep brain stimulation. *J. Neurophysiol.* **120**, 662–680 (2018).
14. Kent, A. R. & Grill, W. M. Neural origin of evoked potentials during thalamic deep brain stimulation. *J. Neurophysiol.* **110**, 826–843 (2013).
15. Escobar, D. *et al.* Parkinsonism and Vigilance: Alteration in neural oscillatory activity and phase-amplitude coupling in the basal ganglia and motor cortex. *J. Neurophysiol.* jn.00388.2017 (2017) doi:10.1152/jn.00388.2017.

16. Devergnas, A., Pittard, D., Bliwise, D. & Wichmann, T. Relationship between oscillatory activity in the cortico-basal ganglia network and parkinsonism in MPTP-treated monkeys. *Neurobiol. Dis.* **68**, 156–166 (2014).

17. Romeo, A. *et al.* Cortical Activation Elicited by Subthalamic Deep Brain Stimulation Predicts Postoperative Motor Side Effects. *Neuromodulation J. Int. Neuromodulation Soc.* **22**, 456–464 (2019).

18. Li, S., Arbuthnott, G. W., Jutras, M. J., Goldberg, J. A. & Jaeger, D. Resonant antidromic cortical circuit activation as a consequence of high-frequency subthalamic deep-brain stimulation. *J. Neurophysiol.* **98**, 3525–3537 (2007).

19. Ljung, L. *System Identification: Theory for the User*. (Prentice-Hall, Inc., 1986).

20. Wilson, C. J. & Bevan, M. D. Intrinsic dynamics and synaptic inputs control the activity patterns of subthalamic nucleus neurons in health and in Parkinson's disease. *Neuroscience* **198**, 54–68 (2011).

21. Bevan, M. D., Magill, P. J., Terman, D., Bolam, J. P. & Wilson, C. J. Move to the rhythm: oscillations in the subthalamic nucleus–external globus pallidus network. *Trends Neurosci.* **25**, 525–531 (2002).

22. Johnson, M. D. & McIntyre, C. C. Quantifying the Neural Elements Activated and Inhibited by Globus Pallidus Deep Brain Stimulation. *J. Neurophysiol.* **100**, 2549–2563 (2008).

23. Buzsáki, G. & Draguhn, A. Neuronal Oscillations in Cortical Networks. *Science* **304**, 1926–1929 (2004).

24. Jirsa, V. & Müller, V. Cross-frequency coupling in real and virtual brain networks. *Front. Comput. Neurosci.* **7**, (2013).

25. Jerome Engel Jr.; Timothy A. Pedley. *Epilepsy: A Comprehensive Textbook*. vol. 1 (Lippincott Williams & Wilkins, 2008).

26. Brown, P. *et al.* Dopamine dependency of oscillations between subthalamic nucleus and pallidum in Parkinson's disease. *J. Neurosci. Off. J. Soc. Neurosci.* **21**, 1033–1038 (2001).

27. Swann, N. C. *et al.* Chronic multisite brain recordings from a totally implantable bidirectional neural interface: experience in 5 patients with Parkinson's disease. *J. Neurosurg.* **128**, 605–616 (2017).

28. Bilateral implantation in globus pallidus internus and in subthalamic nucleus in Parkinson's disease. - PubMed - NCBI. https://www-ncbi-nlm-nih-gov.ezp3.lib.umn.edu/pubmed/22151377.

29. Hashimoto, T., Elder, C. M., Okun, M. S., Patrick, S. K. & Vitek, J. L. Stimulation of the subthalamic nucleus changes the firing pattern of pallidal neurons. *J. Neurosci. Off. J. Soc. Neurosci.* **23**, 1916–1923 (2003).

30. Oppenheim, A. V., Schafer, R. W. & Buck, J. R. *Discrete-time Signal Processing (2Nd Ed.)*. (Prentice-Hall, Inc., 1999).

31. Shannon, R. V. A model of safe levels for electrical stimulation. *IEEE Trans. Biomed. Eng.* **39**, 424–426 (1992).

32. Merrill, D. R., Bikson, M. & Jefferys, J. G. R. Electrical stimulation of excitable tissue: design of efficacious and safe protocols. *J. Neurosci. Methods* **141**, 171–198 (2005).

Figures

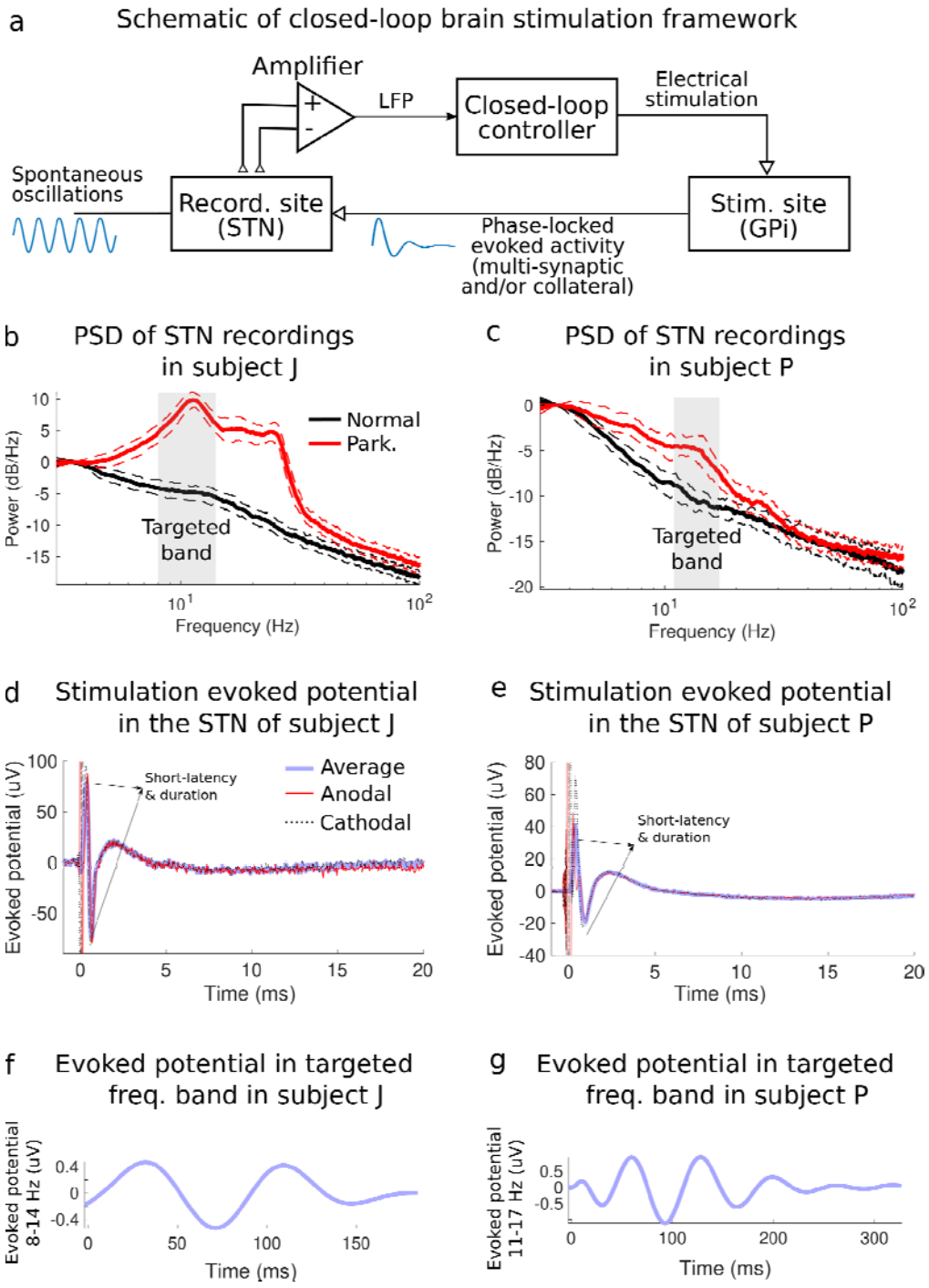

Figure 1. Phase-locked stimulation framework and concept. (a) Schematic of closed-loop neuromodulation framework in which stimulation-evoked activity is used to suppress or amplify spontaneous neural oscillations when stimulations pulses are phase-locked to these

oscillations. The power spectral density (PSD) plots of spontaneous LFP recordings in the STN of the studied animal J and P in the normal and parkinsonian conditions are shown in (b) and (c), respectively. The frequency bands targeted for modulation using phase-locked stimulation are highlighted in gray. These frequency bands have a range of 6 Hz with center frequencies equal to the peak frequency of the PSD plots. Electric potentials in the STN of animal J and P evoked by stimulation pulses in the GPi are shown in (d) and (e), respectively. The evoked potentials displayed in this figure are the average response of a single pulse with an amplitude equal to 600 μA for animal J and 800 μA for animal P. Short-duration and short-latency evoked oscillations, depicted in (d) and (e), are associated with antidromic neural activation of the STN following the stimulus pulse. (f,g) Stimulation-evoked potentials in the targeted frequency bands for animal J and P are shown. The potentials in (f,g) illustrate the evolution of oscillations evoked by a single stimulation pulse in the frequency bands targeted for modulation using phase-locked brain stimulation, responsible for the modulation observed when phase-locked stimulation is delivered. Note that the time scale of the evoked potentials shown in (f-g) is different to that shown in (d-e).

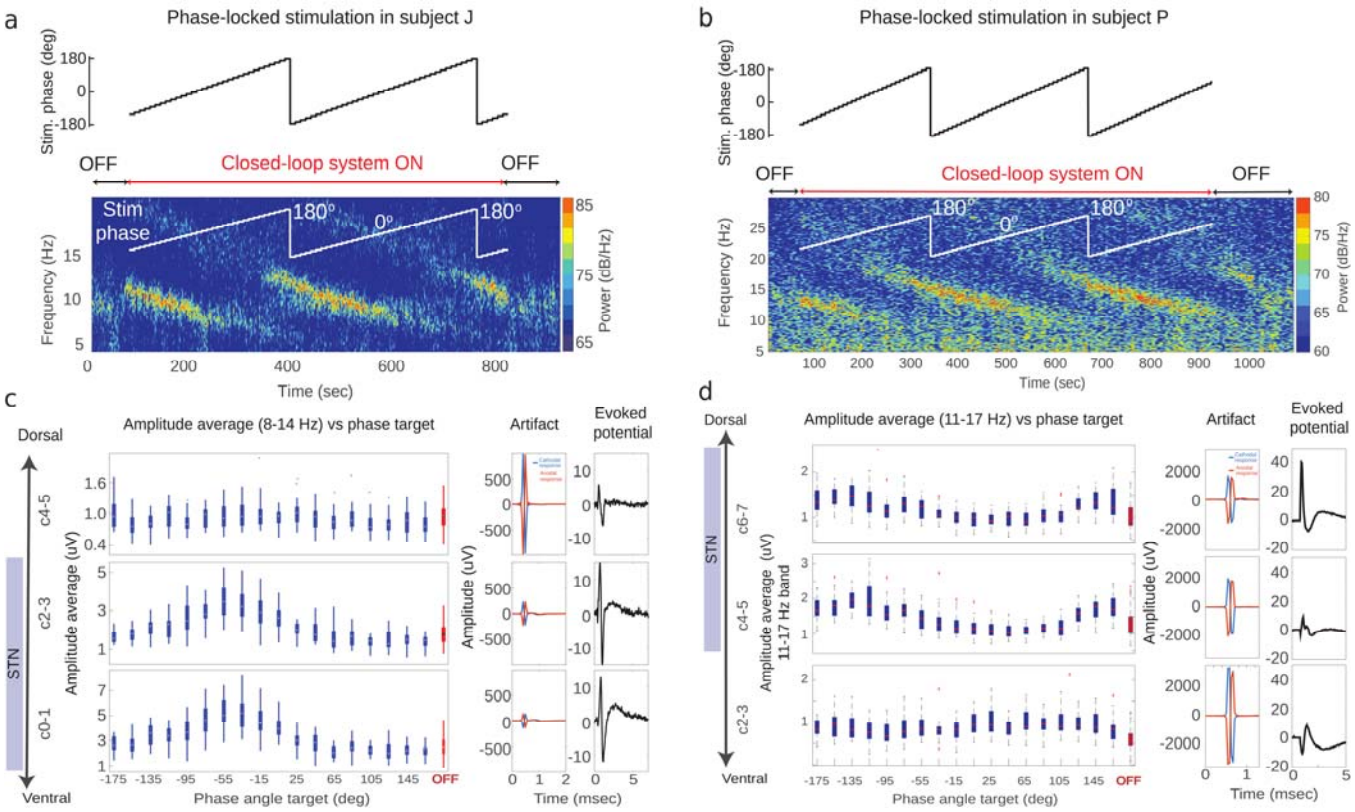

Figure 2. Amplitude of oscillations as a function of stimulation phase. (a, b) Results of experiments in which phase-locked stimulation was tested in animal J and P. The targeted (reference) phase angle for stimulation was varied by 10 degrees every 10 seconds, while the stimulation current delivered to the GPi was fixed at 600 μA in both animals. Spectrograms illustrating the power over time and frequencies for different phase angles in the OFF and ON stimulation state are shown in (a) and (b) for animal J and P, respectively. The spectrograms show data recorded using electrode pairs used to implement the closed-loop stimulation algorithm. The amplitude of neural oscillations as a function of the targeted phase angle and across electrode pairs is shown for animal J and P in (c) and (d), respectively. Electrodes C0-C2 in animal J and C4-C6 in animal P used for sensing are located within the STN. The artifacts and evoked potentials computed across electrode pairs are shown in (c) and (d) (center and right columns). Evoked potentials were calculated based on stimulation-triggered averages of LFPs by using both cathodal and anodal stimulation ($X_a(t)$ and $X_c(t)$). These evoked potentials were calculated as $((X_a(t) + X_c(t))/2)$.

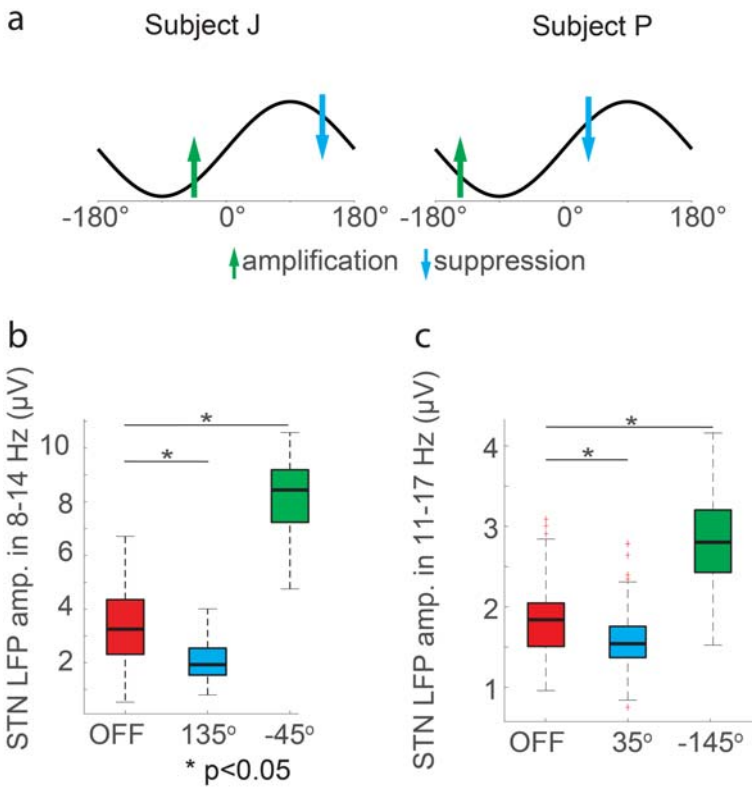

Figure 3. Differences between the amplitude of oscillations when stimulation was OFF and when stimulation was delivered at the phase angles associated with maximum suppression/amplification. (a) Schematic of phase angles at which stimulation was delivered to achieve maximum suppression (blue arrow) or amplification (green arrow) of neural oscillations in the 8-14 Hz band for animal J and 11-17 Hz band for animal P, respectively. (b) Box plots illustrating the interquartile ranges and medians of 1-second segments of the amplitude envelope of LFP data filtered in the targeted frequency band in the OFF stimulation state and when stimulation was delivered at phase angles that achieved maximum suppression and amplification of oscillations. We assumed that the difference between measurements in the two conditions was significant when $p < 0.05$. The p-values resulting from this test were corrected for the number of comparisons via the Bonferroni method. The number of data segments (n) the in the OFF stimulation, amplification, and suppression

conditions for animal J were 143, 27, and 18, respectively; for animal P these numbers were 150, 20, and 20, respectively. The boxplots were created based on data from the experiment illustrated in **Fig. 2**.

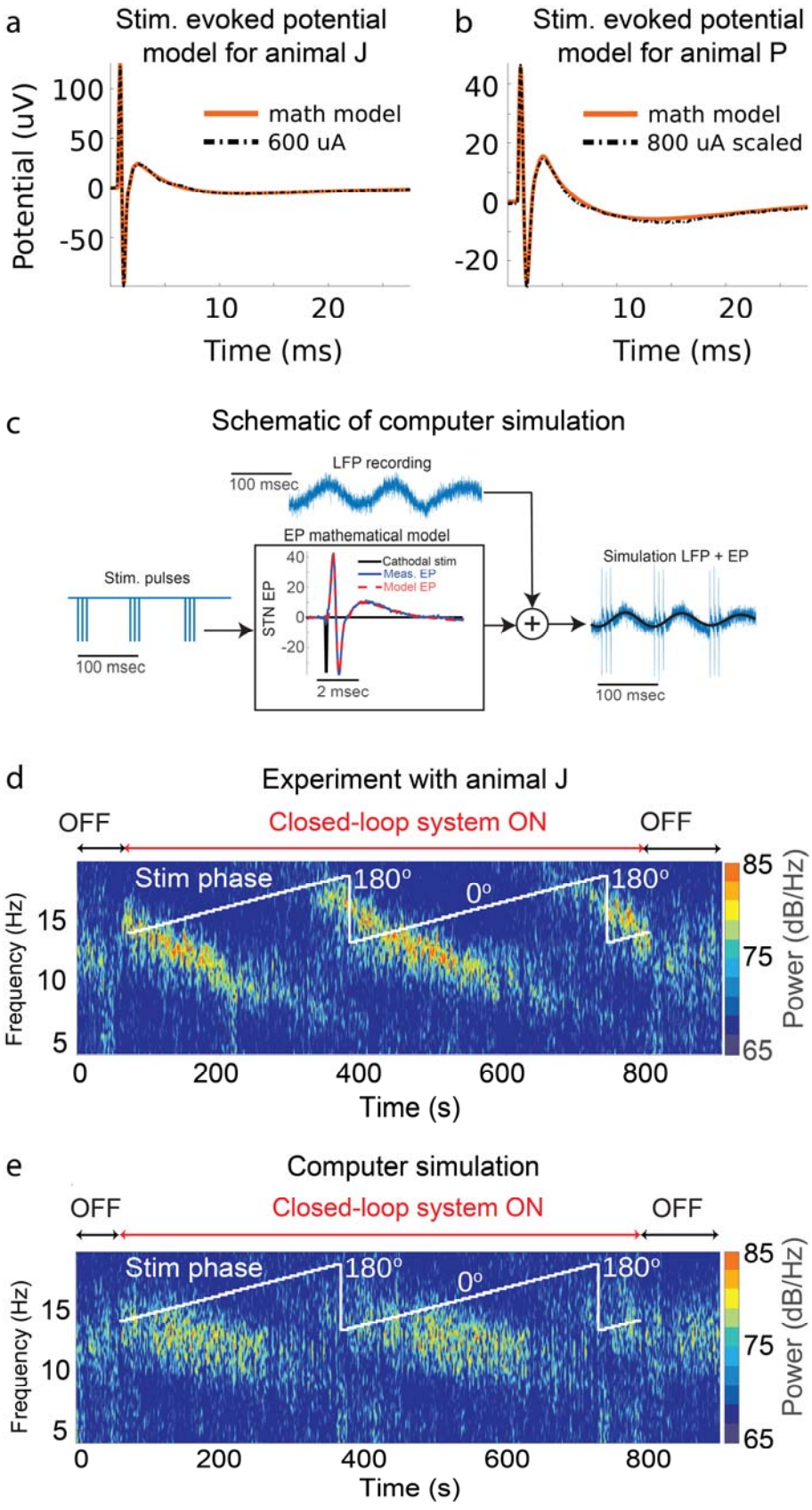

Figure 4. Computer simulations of phase-locked stimulation. (a, b) Stimulation-evoked

potentials calculated using experimental data together with their corresponding mathematical models. The evoked potential mathematical models are computed through the convolution of an evoked potential transfer function obtained via system identification techniques and the stimulation pulse mathematical function. (c) Schematic of computer simulation in which pre-recorded or computer-generated (synthetic) oscillations are added to the evoked potential (EP) time series to model the steady-state of modulated oscillations. The evoked potential time series is computed through the mathematical model with an input equal to stimulation pulses phase-locked to the oscillations in the selected frequency band. (d) Experimental data with animal J in which phase angles were varied over time. (e) Computer simulation of phase-locked stimulation created using STN LFP data (stimulation-free) from animal J and mathematical models of the stimulation-evoked potentials. The targeted phase angles in both experiments and computer simulation were varied over time, increasing the phase angle by ten degrees each ten seconds.

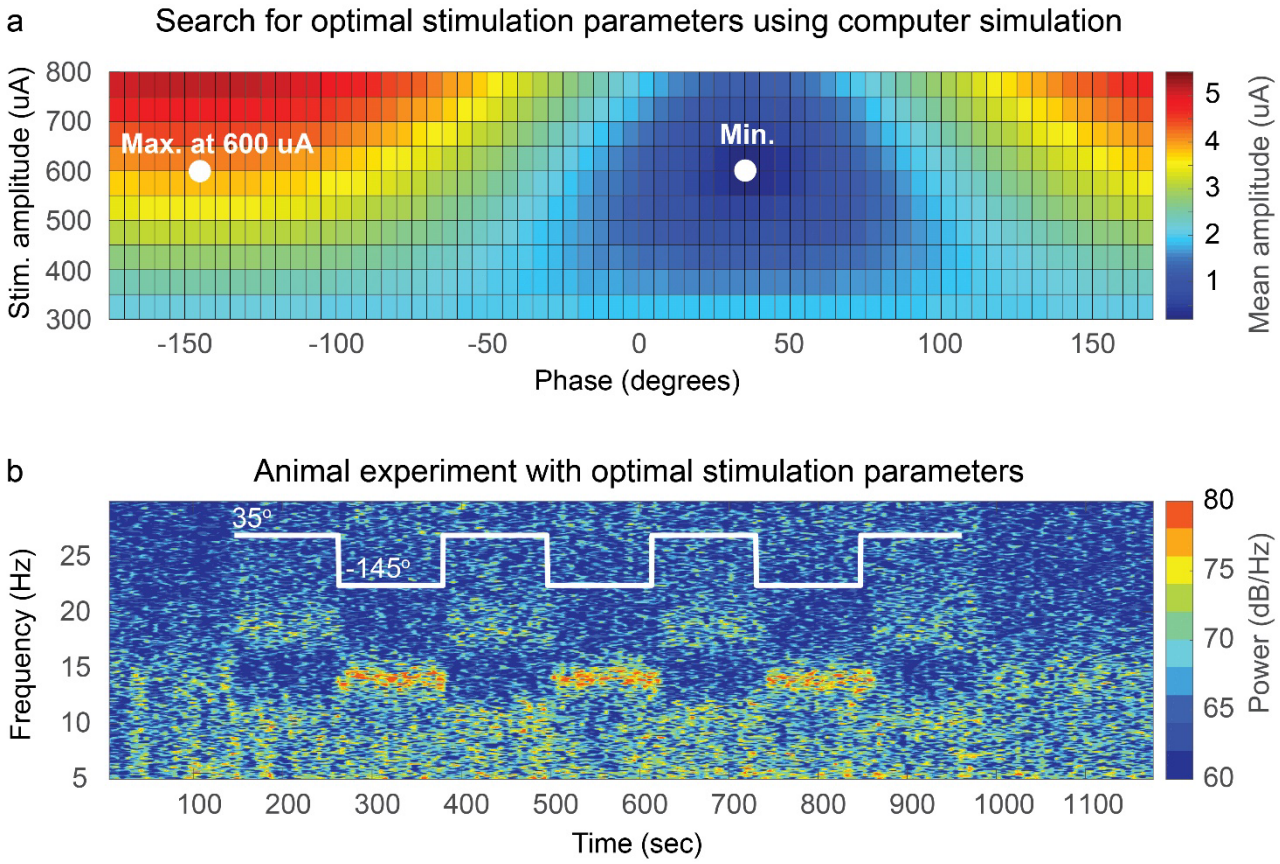

Figure 5. Optimization of stimulation parameters. (a) Optimization map to estimate optimal stimulation amplitudes and phases to suppress/amplify neural oscillations in the 11-17 Hz band with a mean amplitude of 1.95 μA in animal P by using phase-locked stimulation. The color scale represents the mean amplitude of oscillations created in computer stimulations at different stimulation phases and amplitudes. The optimal phase and amplitude to suppress oscillations were found to be 35 deg and 600 μA, respectively. (b) Spectrogram of STN LFP data in which phase-locked stimulation was delivered at stimulation amplitude found to be optimal for suppression of 11-17 Hz oscillations (600 μA). The stimulation phase was alternated between the optimal phase for suppression and the optimal phase for amplification at 600 μA, which is illustrated with the white curve on the spectrogram. The recordings shown in this figure are from the electrode pair that was used for sensing in the closed-loop stimulation system.